Diagnostic Pathology: Open Access
ISSN: 2476-2024

Rossi S et al. Diagn Pathol Open 2018, 3:1
DOI: 10.4172/2476-2024.1000132

Research Article Open Access

Description of an Intracellular Stage in the Experimental Infections of Albino Mice with a Venezuelan Isolated of *Trypanosoma evansi* Using Scanning and Transmission Electron Microscopy Techniques

Marcello S. Rossi S.[1,2]*, Alpidio Alejandro Boada-Sucre[3], María Lorena Márquez[2], Pedro Rodríguez[4], María Gilma Hernández[5], Francisco García[6,†], Gilberto Payares[2], and Héctor J. Finol[4]

[1]*Laboratorio de Arbovirus y Enfermedades Virales Emergentes, Centro Nacional de Microbiología, Instituto de Salud Carlos III, Madrid, España*
[2]*Laboratorio de Inmunología y Quimioterapia, Instituto de Biología Experimental (IBE), Facultad de Ciencias, Universidad Central de Venezuela (UCV), Caracas, Venezuela*
[3]*Laboratorio de Microscopía Electrónica, Instituto de Estudios Científicos y Tecnológicos (IDECYT), Universidad Nacional Experimental Simón Rodríguez (UNESR), Caracas, Venezuela*
[4]*Centro de Microscopía Electrónica "Mitsuo Ogura", Facultad de Ciencias, Universidad Central de Venezuela (UCV), Caracas, Venezuela*
[5]*Instituto de Biomedicina y Ciencias Aplicadas (IIBCA), Universidad de Oriente (UDO), Cumaná, Venezuela*
[6]*Cátedra de Parasitología, Facultad de Ciencias Veterinarias,Universidad Central de Venezuela (UCV), Caracas, Venezuela*

Abstract

In Venezuela *Trypanosoma evansi* is responsible for trypanosomosis that affects equines, canines, bovines and wild animals such as capybaras. The pathology of the infections by this monomorphic trypanosome has been extensively studied by different authors in experimental and field conditions at level of light and electron microscopy. The aim of this study is to provide additional evidences about the development of an intracellular stage during experimental infections of albino mice with a Venezuelan isolated from Apure state. Samples of different organs from mice experimentally infected with 10^4 trypanosomes were prepared for transmission and scanning electron microscopy. Results show the presence of *T. evansi* in the lumen of blood vessels and interacting with endothelial cells, Küpffer cells, macrophages, lymphocytes and neutrophils. A frequent finding was the detection of intracellular trypomastigotes in the cytoplasm of normal looking and necrotic cells of the adrenal cortex, liver, capillaries and spleen. Despite most of the intracellular trypomastigotes observed, presented the ultrastructural feature of trypomastigotes from subgenus *Trypanozoon*, only a very few number of trypanosomes showed an ultrastructure compatible with an epimastigote-like. Most of trypanosomes presented a normal ultrastructure, however ultrastructural patterns suggestive of apoptosis could also be evidenced. Results are discussed in the context of their impact in the diagnosis, treatment of the disease, evasion of immune system, immunosuppression as well as the persistence and prevalence of *T. evansi* in natural hosts.

Keywords: Experimental infection; Mice; *Trypanosoma evansi*; Venezuelan isolated; EcHF91; Intracellular stages; Trypomastigotes; Epimastigotes-like; Apoptosis; SEM; TEM

Abbreviations: AAT: African Animal Trypanosomosis; VAT's: Variant Antigen Types; CNS: Central Nervous System; Isolated EcHF91: Isolated from *Equus caballus* at the Hato el Frío (Venezuela) on 1991; TEM: Transmission Electron Microscopy; SEM: Scanning Electron Microscopy; PCR: Polymerase Chain Reaction; PBS: Phosphate buffered Saline; NMRI-IVIC: Naval Medical Research Institute-Instituto Venezolano de Investigaciones Científicas; IP: Intraperitoneal; OS: Overall Survival; Pa: Pascal; CO_2: Carbon dioxide; Tryp: Trypanosomes; SER: Smooth Endoplasmic Reticulum; RER: Rough Endoplasmic Reticulum; *HhHF92*: Isolated from *Hydrochoerus hydrochaeris* at the Hato el Frío (Venezuela) on 1992; *EcM96*: Isolated from *Equus caballus* at Mantecal (Venezuela) on 1996; kDa: Kilodalton; CHO: Chinese Hamster Ovary cells; PIP3: Phosphoinositol Triphosphate; Ca^{2+}: Calcium cation; ITS1: Internal Transcribed Spacer 1; *TEVA1*: *Trypanosoma evansi* strain 1; LDLr: Low Density Lipoprotein receptor; FONACIT: Fondo Nacional de Ciencia, Tecnología e Innovación; IBE-UCV: Instituto de Biología Experimental-Universidad Central de Venezuela; DSc: Doctor of Science.

Introduction

Trypanosomosis is a complex of diseases that affect man and his livestock in Africa, Asia, Central and South America. The African Animal Trypanosomosis (AAT) caused by *Trypanosoma brucei*, *Trypanosoma evansi*, *Trypanosoma vivax*, *Trypanosoma congolense* and *Trypanosoma simiae* is probably the more serious problem for the development of the region, because more than 44 million of cows are at risk of dying in the sub-Saharan Africa [1,2], a problem that worsens when more than 55 million people are considered to be at risk of contracting sleeping-sickness [3]. The losses associated to inefficient control of AAT were estimated in US$1340 million per year, without including indirect livestock benefits such as manure, traction and secondary products such as clothing and hides. In addition, losses in terms of meat and milk productivity alone have been calculated in US$700 million per year [1]. In South America the impact of domestic animals trypanosomosis caused by *T. evansi* has not been satisfactorily estimated and no financial estimates are available for countries such as Venezuela.

In Venezuela animal trypanosomosis is mainly caused by *T. vivax* and *T. evansi*. Regarding to *T. evansi*, it is well known that is the

***Corresponding author:** Marcello S. Rossi S, Laboratorio de Arbovirus y Enfermedades Virales Emergentes, Centro Nacional de Microbiología, Instituto de Salud Carlos III, Madrid, España, Tel: 0034-911265512; E-mail: rossimarcell@gmail.com

Received July 01, 2017; **Accepted** January 22, 2018; **Published** January 24, 2018

Citation: Rossi SMS, Boada-Sucre AA, Márquez ML, Rodríguez P, Hernández MG, et al. (2018) Description of an Intracellular Stage in the Experimental Infections of Albino Mice with a Venezuelan Isolated of *Trypanosoma evansi* Using Scanning and Transmission Electron Microscopy Techniques. Diagn Pathol Open 3: 132. doi: 10.4172/2476-2024.1000132

etiological agent of equine trypanosomosis known as "Derrengadera" [4] with high seroprevalence rates especially in geographic locations where it is enzootic such as the Apure State (81.7%) [5]. The transmission of the infection is carried out by biting flies of Tabanidae family [6-8], affecting horses, donkeys, bovines [9,10] and wild animals as capybara (*Hydrochoerus hidrochaeris*) in which it causes a subpatent or asymptomatic infection [11]. Recently, human infections caused by *T. evansi* have been reported in India [12,13] and southern Vietnam [14]. Although these infections are associated with a lack of apolipoprotein L-I, the number of cases could be underestimated. For these reasons, the evaluation and improvement of new diagnostic tests and field researches are required for detection and confirmation of these atypical cases [15].

Infections caused by *T. evansi* in domestic animals can be acute with fever, emaciation, anemia and sudden death in some cases or chronic, with a progressive weakness, emaciation and a notable decrease in the productive capacity [16]. The pathology of *T. evansi* infections has been extensively studied by different authors in experimental and field conditions [17-23]. As a consequence of its location inside host body, *T. evansi* has been included together with *T. brucei*, *T. brucei rhodesiense*, *T. brucei gambiense*, *T. equiperdum* and *T. cruzi*, within a trypanosome-group whose infection occurs in the blood plasma, but may also occur extravascularly and in certain body fluids (cerebrospinal fluid, peritoneal and synovial liquids and aqueous humor), triggering not only anemia, but also extensive inflammatory, necrotic and degenerative processes [24].

Our electron microscopic studies about the ultrastructural pathology of the murine infections with *T. evansi* were able to detect trypomastigotes in the blood vessels of all tissues studied in adrenal cortex [25], skeletal muscle [26], liver [27], spleen, kidneys and testes, as well as in the connective tissues of liver and adrenal gland. The extravascular presence of *T. evansi* should not constitute a new surprising fact, because the very first extravascular observation of trypanosomes from brucei-group (*T. brucei*, *T. brucei rhodesiense*, *T. brucei gambiense*, *T. evansi* and *T. equiperdum*), was made in 1912 by Wolbach and Binger, who described that the infections with these trypanosomes cause severe damages in the perivascular connective tissue, characterized by disorganization and breaking of collagen bundles, as well as fibroblasts destruction [28].

Luckins et al. [19] recognize the presence of *T. evansi* in the connective tissues of the skin from rabbits experimentally infected and propose that the extravascular location of the trypanosomes at the site of inoculation should be responsible for the aggressive inflammatory response, with collagen destruction, edema and necrosis. In addition, they proposed that the extravascular growth of the trypanosome populations and the consequent increase in the number of variant antigen types (VAT´s), would allow the colonization of the bloodstream by *T. evansi*, as a consequence of the evasion of host immune system through the mechanism of antigenic variation.

Similar observations were described by Uche and Jones [20] in the spleen, lymphatic nodes, vulva and ears of experimentally infected rabbits, and Biswas et al. [23] in the liver of Bandicoot rats. These results confirm that the presence of extravascular trypomastigotes in kidneys, heart, lungs, liver, and central nervous system (CNS), instead to constitute indicators of a protective immune response, constitute a destructive response capable to cause hosts death. The abundance of these extravascular forms of *T. evansi* during the experimental and natural infections besides being responsible for the higher mortality for deer (*Cervus porcinus*) [18,22], could be associated to the genetic predisposition of the host to the infection and the development of an inadequate immune response among other factors

As it has also been described for *T. brucei*, the extravascular presence of *T. evansi* could be a consequence of the ultrastructural damage observed in the capillary, arterioles and veins of the infected animals. Damage to the vasculature described for the infection of the adrenal glands [25], skeletal muscle [21,26,29] and liver [27] with the same Venezuelan isolate of *T. evansi* , were severe enough to allow the infiltration of blood cells, trypomastigotes but also biologically active molecules secreted by live *T. evansi* trypomastigotes [30] or from dead trypanosomes into tissues and extravascular spaces.

The main contribution of this work is the confirmation that the occurrence of intracellular stages in experimental infections of albino mice with the Venezuelan isolated EcHF91 of *T. evansi* is more frequent than what was initially reported in the preliminary works of our group [25-27,29]. In this regard extensive observations of a greater number of ultrathin sections allowed us to verify that cell invasion is not only limited to cells of the adrenal cortex, hepatocytes and vascular endothelium, but also to cells of the immune system such as plasma cells and lymphocytes. In addition, the ultrastructural and morphological findings obtained by Transmission Electron Microscopy (TEM) and Scanning Electron Microscopy (SEM) provide suggestive evidence on the occurrence of an active invasion process as well as the confirmation that bloodstream and intracellular trypomastigotes share the same ultrastructural features. The results are discussed in the context of the impact of these stages on the diagnosis-treatment of *T. evansi* trypanosomosis, its evasion of immune system, the persistence of this hemoparasite in natural hosts as well as its seroprevalence and detection by the polymerase chain reaction technique (PCR) in clinical and parasitological healthy animals.

Material and Methods

Trypanosoma evansi

The population of *T. evansi* used in this work was derived from a heterogeneous line originally isolated in 1991 from an infected horse (*Equus caballus*) at the Hato El Frío (7° 56' North and 68° 57' West) in the Apure State of Venezuela (Ec/1991/Faculty of Veterinary Sciences-UCV/Stock 3/IBE). This heterogeneous population (EcHF91) was classified as *T. evansi* according to the clinical manifestations, its morphology, parasitological behaviour and ultrastructural feature (low number of coated vesicles in the flagellar pocket in relation to *T. equiperdum* a co-endemic specie of trypanosome) [31]. It was maintained in the laboratory through passages in albino rats and cryopreservation at -196°C, using 1% glucose PBS pH 7.4 with 10% (v/v) dimethyl-sulphoxide as cryoprotector.

Experimental design and infections

Two groups of 10 heterozygous male mice (NMRI-IVIC) with a body weight of 20-25 g were used for the electron microscopic and parasitological studies. They were kept in metal cages, using rice-shell as a bed in the animal facility of the Laboratory of Immunology and Chemotherapy (Instituto de Biología Experimental-UCV). They were fed on Ratarina® and ozonized water ad libitum, and experimentally infected by intraperitoneal (IP) inoculation with 0.1 ml of diluted rat infected blood containing 10^4 trypanosomes (400 trypanosomes/g of body weight). Parasitaemia of both groups was daily checked as described by Brener method [32] and 6 animals for electron microscopic studies were sacrificed on day 5 post-infection under Ketamine anesthesia (80-120 mg/kg IP), when they were dying and parasitaemia reached levels

of approximately 10^9 trypanosomes/ml. A third group of healthy mice (n=4) were also sacrificed and used as controls.

The overall survival (OS) of groups was defined as the number of live mice present in the cages at each day. All the dying mice (in a convulsing and prostrated state with nose-bleeding) present in cages were euthanized under anesthesia as previously described in order to avoid their suffering.

Statement of animal rights

During experimental infection, all animals were maintained under veterinary supervision to safeguard health and minimize animal suffering. Protocols used were approved by the Ethical Committee for Laboratory Animal Use under number 013-11 according to the Ethics Chart of animal experimentation.

Electron Microscopy

Transmission electron microscopy

Pieces of adrenal glands, liver and spleen (2 mm^3 each) were fixed with Karnovsky´s solution (2.5% glutaraldehyde, 4% *p*-formaldehyde in 0.1 M Millonig phosphate buffer pH 7.4) and 1% osmium tetroxide, dehydrated in increasing ethanol concentrations and embedded in LX-112 epoxy resin (Ladd Research Inc., Burlington) according to Rossi et al. [25]. Ultrathin sections were obtained with a diamond knife in a Porter-Blum MT2-B ultramicrotome, stained with uranyl acetate and lead citrate [33], and examined with Hitachi models H500 and H7100 transmission electron microscopes with an acceleration voltage of 75-100 kV.

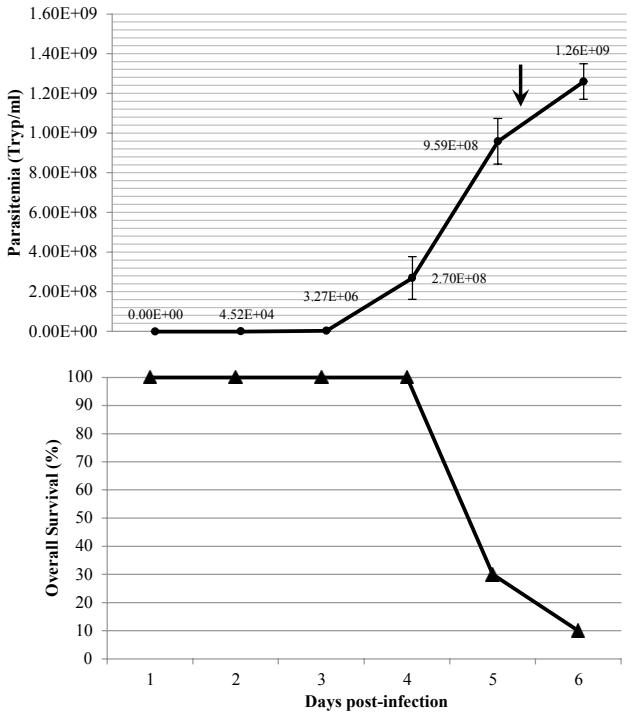

Figure 1: Parasitaemia and overall survival of mice experimentally infected with *T. evansi.* Parasitaemia calculations were performed with (n=20) mice from both experimental groups. The black arrow (↓) indicates the time when the animals were sacrificed for the electron microscopic study. The bars represent the standard deviation of the parasitaemia mean calculated at each point with (n=20) mice from day 1 to 4 post-infection, (n=6) mice on day 5 and (n=2) mice on day 6 post-infection.

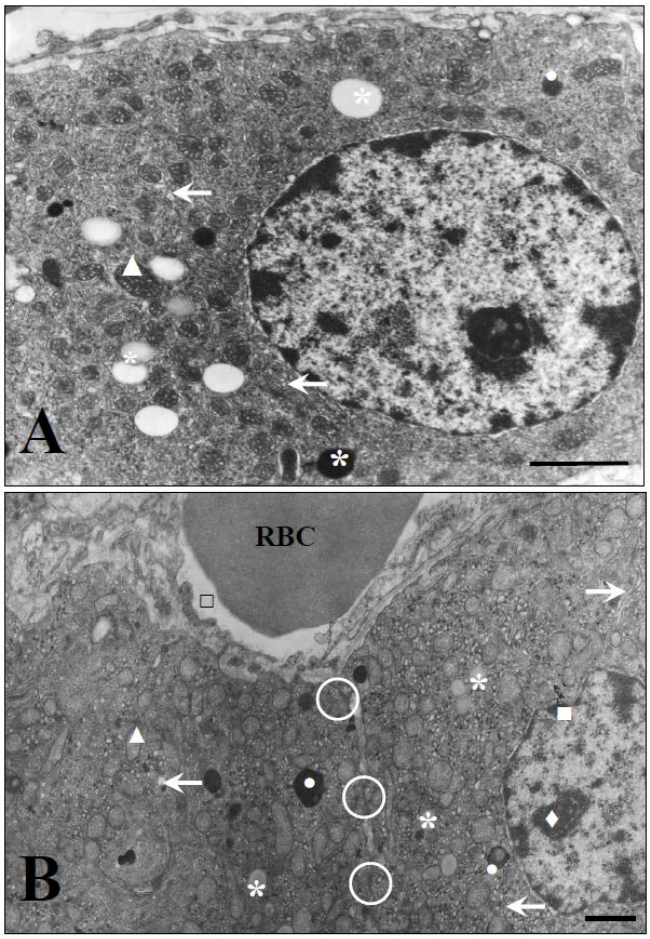

Figure 2: Normal ultrastructure of cells from adrenal glands of healthy mice. **(A)** Cortical cell from fasciculate layer characterized by their characteristic mitochondria with tubular cristae (white ▲). Notice the presence of lipid droplets (white*), tubular SER (white →) and some lysosome (White●). Bar: 1.5 µm. **(B)** Cortical cells from reticularis layer showing the abundance of mitochondria with vesicular cristae (white ▲), lipid droplets (white*), SER (white →), some lysosome (white ●) and the union complexes (○) between two contiguous cells. (■) nucleus; (♦) nucleolus; (RBC) erythrocyte; (□) capillary lumen. Bar: 1.4 µm.

Scanning electron microscopy

Pieces of the aforementioned organs were fixed and freeze fractured. Briefly, tissue pieces were fixed with Karnovsky´s solution, cryoprotected by incubation with 25% (v/v) glycerol in 0.1 M Millonig phosphate buffer pH 7.4 for 45 minutes at ambient temperature and quickly frozen under super cooled isopropane (-196°C). Frozen samples were freeze-fractured with a steel knife in a JEOL 9010C freeze-fracture device (1×10^{-6} Pa, -120°C), dried by evaporation on a critical point dryer (Hitachi HCP-2) using carbon dioxide (CO_2) as liquid transition fluid, mounted on a sample holder and shadowed with platinum ions (Electron Microscopy Science EMS-350) [34]. Microscopic observations were done with Hitachi model S800 scanning electron microscope with an acceleration voltage of 5 kV.

Results

The course of parasitaemia of mice experimentally infected with *T. evansi* is shown in Figure 1. The prepatent period was 2 days and maximal parasitaemia (1.26×10^9 Tryp/ml) was reached when the overall survival of both experimental groups was 10% (1 out of 10 mice).

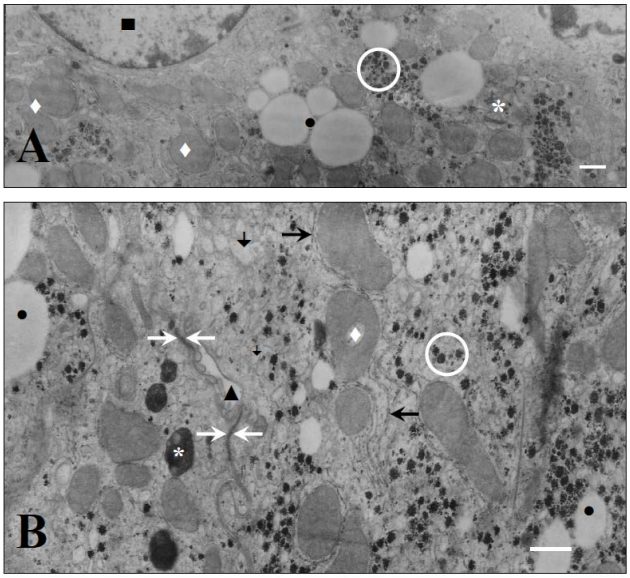

Figure 3: Transmission electron micrographs of liver from healthy mice at different magnifications showing the normal ultrastructure of hepatocytes. In **(A)** it can be seen that hepatocytes are cells rich in mitochondria (white ♦), lipid droplets (●) and glycogen particles (○). The presence of some microbodies (White*) is also seen. Bar: 1.2 µm. **(B)** Notice the presence of a bile canaliculus with its microvilli (▲) as well as the union complexes (→←) between two hepatocytes and the abundance of lysosomes (white*), RER (black →) and tubular SER (*). (■) hepatocyte nucleus. Bar: 2 µm.

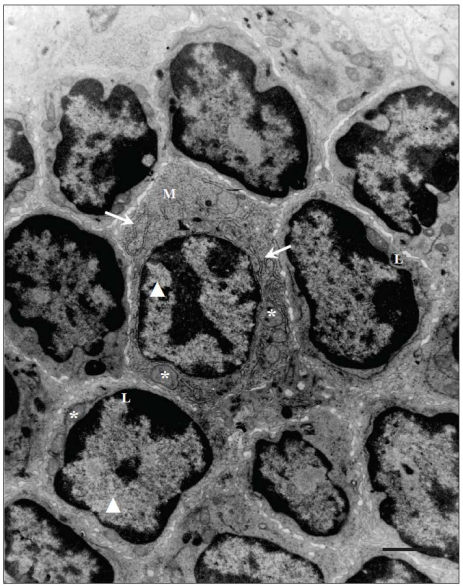

Figure 4: White pulp of spleen from healthy mice showing the abundance of lymphocytes (L) in close contact with them and interacting with a macrophage (M). (White*) mitochondria; (▲) cells nuclei; (→) RER. Bar: 1.8 µm.

Figures 2-4 show the normal ultrastructure of the adrenal cortex cells, hepatocytes and spleen white pulp from the healthy mice used as controls respectively. As it can be seen in Figure 2, cortical cells from fasciculate layer showed the normal ultrastructure of steroid producing cells characterized by abundant mitochondria with tubular (Figure 2A) or vesicular (Figure 2B) cristae, a well-developed tubular smooth endoplasmic reticulum (SER) and lipid droplets.

Transmission electron micrographs obtained from hepatocytes of healthy mice (Figure 3), showed the normal ultrastructural feature of cells with high metabolic function as judged by the abundance of mitochondria, rough endoplasmic reticulum (RER) and SER, lysosomes, glycogen particles and lipid stores (lipid droplets) (Figures 3A and 3B). Normal bile canaliculi between hepatocytes were also seen (Figure 3B).

White pulp from control mice (Figure 4) showed numerous lymphocytes (characterized by their high ratio nucleus/cytoplasm), in close contact between them and macrophages, while the spaces in red pulp (results not showed) contained lymphocytes, reticular cells, erythrocytes and platelets.

The presence of bloodstream trypomastigotes during the experimental infection of mice with *T. evansi* (EcHF91) was demonstrated in different host organs compartments. A frequent finding was the presence of bloodstream trypomastigotes in the lumen of the blood vessels of the adrenal cortex (Figure 5), as well as in the liver sinusoids (Figures 6A and 6B) and splenic sinuses (Figures 7A and 7B).

Bloodstream forms of *T. evansi* were also frequently observed interacting with the surface of Küpffer cells (Figure 6B), endothelial cells in the adrenal cortex (Figures 5 and 8), hepatic sinusoid walls (Figure 6B, 9A and 9B), or phagocytosed by endothelial cells (Figure 10A) or neutrophils (Figure 10B).

A peculiar and frequent finding was the observation of intracellular *T. evansi* trypomastigotes inside remains of cells of the adrenal cortex (Figure 11A) as well as inside cells showing cytoplasm of normal looking ultrastructure (Figure 11B). No intracellular trypomastigotes were observed in adrenal medulla (results not showed). In the liver, intracellular trypanosomes were detected inside the cytoplasm of normal (Figure 12) and necrotic hepatocytes (Figures 13 and 14).

The presence of intracellular trypomastigotes was not limited to

Figure 5: Transmission electron micrograph of a blood vessel from the adrenal cortex (Bar: 0.5 µm) of mice experimentally infected with *T. evansi*. Notice the presence of a bloodstream trypomastigote (T) with their characteristic flagellum (F), mithocondrion and kinetoplast (*), close to endothelial cell (■) cytoplasm extensions (→ ←) and interacting with cell through flagellum. In the adrenal cortical cells lipid droplets (♦) and mitochondria (▲) can be seen. (○) Mitochondria in endothelial cell can be also seen.

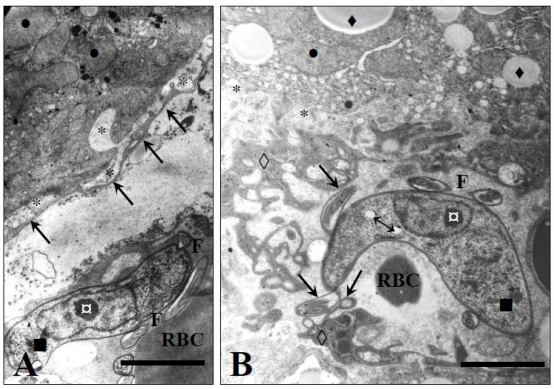

Figure 6: Bloodstream trypomastigotes of *T. evansi* (■) in a liver sinusoid **(A)** showing the endothelial wall **(→)** and **(B)** showing the interaction of a flagellate with a sinusoidal lining Küppfer cell (◊) forming the sinusoidal wall. Notice the prominent nucleolus of *T. evansi* (¤). (↔) acidocalcisomes (previously known as polyphosphate vacuoles); (●) hepatocyte mitochondria; (♦) lipid droplets; (*) Disse's space; (F) flagellum; (RBC) Red Blood Cell. Bar: 1.2 µm.

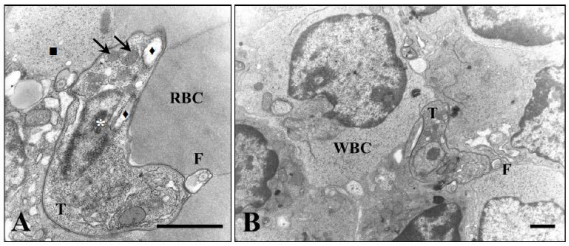

Figure 7: Spleen of mice experimentally infected with *T. evansi*, showing **(A)** a trypomastigote close to red blood cells (RBC) and a reticulocyte (■) in the red pulp (Bar: 1.2 µm) and **(B)** in the white pulp surrounded by white blood cells (WBC) (Bar: 0.5 µm). (T) bloodstream trypomastigotes; (F) flagellum; (→) glycosomes; (♦) mitochondrion; (White*) nucleolus.

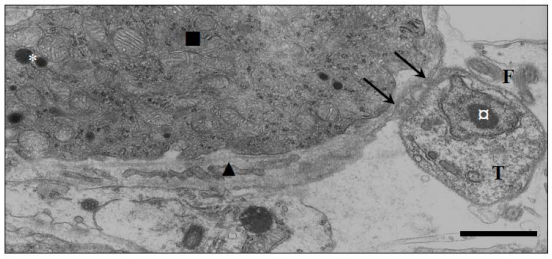

Figure 8: Transmission electron micrograph of the interaction of a *T. evansi* bloodstream trypomastigote (T) with the endothelial cell (▲) of a blood vessel in the adrenal cortex of experimentally infected mice. The close association between the cell body of trypanosome and the endothelial wall is shown (→). (■) cell of the adrenal cortex; (white*) lysosomes; (¤) trypanosome nucleolus. Bar: 1.5 µm.

the adrenal cortex and liver parenchyma; they have been also detected less frequently inside plasma cells (Figure 15), endothelial cells of blood vessels from adrenal cortex (Figure 10A) and interacting with large activated spleen lymphocytes.

These intracellular stages of *T. evansi* showed to have the same ultrastructural feature of bloodstream trypomastigotes, with the exception of some forms observed in liver (Figure 14). These forms showed an ultrastructure that resembles the epimastigote stage of African trypanosomes, as judged for the position of the kinetoplast in relation with the anterior body end. Additionally, intracellular trypanosomes described were not inside a parasitophorous vacuole, appearing freely in the cytoplasm surrounded by lipid droplets, mitochondria, glycogen particles and RER (Figures 11A, 11B, 12-14, 15A).

Although in most of the electron micrographs herein presented (Figures 5, 6A, 6B, 7A, 7B, 8, 13 and 14), the ultrastructure of the *T. evansi* trypomastigotes was normal, as judged by comparisons with findings reported by Hernández-Páez [35], the ultrastructure of trypomastigotes in some electron micrographs (Figure 10A, 11A, 11B and 15), resembles the ultrastructural feature of *T. brucei* cell-death, characterized by apoptotic ultrastructural features such as swollen mitochondrion (Figures 10A, 15A and 15B), an apparent increase in glycosome electron density (Figures 11A and 11B), an apparent decrease on cytoplasm electron density (loss of cytoplasmic material) (Figure 15A), and alteration of nuclear chromatin (Figure 15B).

As it will be discussed in the next section, a working hypothesis

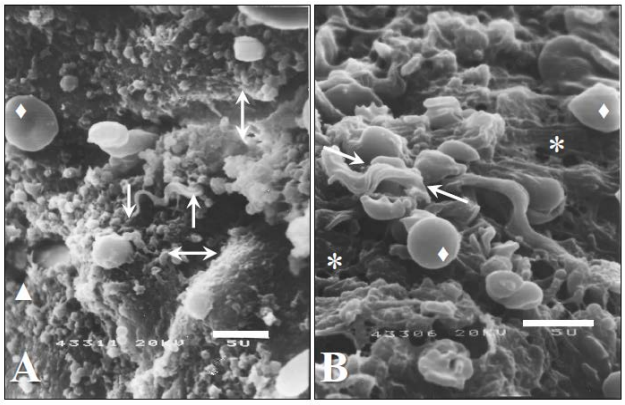

Figure 9: Scanning electron micrography of a liver freeze-fracture preparation showing **(A)** the interaction of bloodstream trypomastigotes of *T. evansi* (white→) with a sinusoid wall (white↔) through its posterior end and **(B)** suggesting the penetration of the sinusoidal wall by a *T. evansi* trypomastigote through its anterior end (white→←). The electron micrographs also show the microvilli of hepatocytes extended into the Disse's space (white▲), the presence of fenestrations (white*) and the discontinuity of the sinusoid walls. Notice the undulating membrane of the *T. evansi* trypomastigote in **(B)**. (♦) red blood cells. Bar: 5 µm

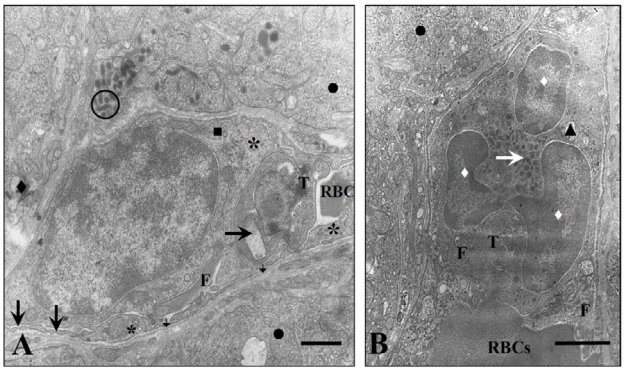

Figure 10: Phagocytosis of *T. evansi* bloodstream trypomastigotes (T) by **(A)** an endothelial cell (■) from a capillary (Bar: 0.7 µm) and **(B)** a neutrophil (▲) inside the blood vessels of the adrenal cortex (Bar: 1.0 µm). In **(A)** notice the fenestrae (↓) and cytoplasm of endothelial cell (*), trypanosome mitochondrion (→); the basement membrane of capillary (ˈ) and microvilli (black ♦) of cortical cell (●). (○) lysosomes; (RBCs) red blood cells; (white ♦) nuclear lobes; (→) neutrophil granules.

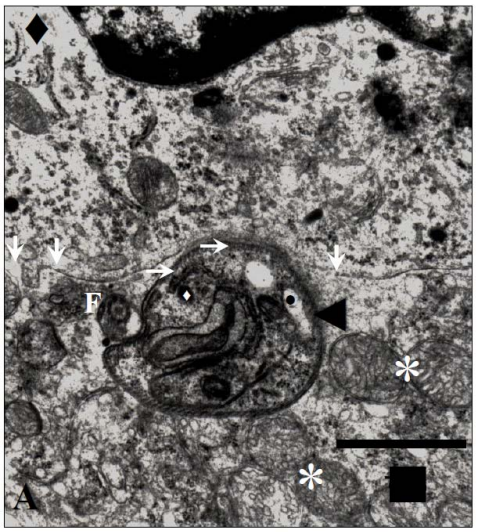

Figure 11A: Intracellular form of *T. evansi* (◄) inside remains of a cell of the adrenal cortex (■) surrounded by mitochondria (white*). Notice that adrenal cortex cell is interacting with a necrotic white blood cell (♦) judging by the loss of plasma membrane integrity (white ↓). (●) trypanosome mitochondrion; (white F) flagellum; (white ♦) glycosome; (white →) oblique sections of subpelicullar microtubules. Bar: 0.8 µm.

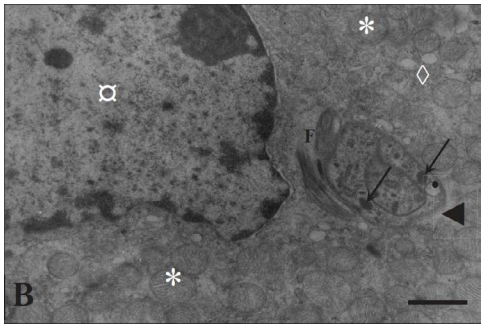

Figure 11B: Intracellular trypomastigote of *T. evansi* (◄) in the cytoplasm of a normal looking cortical cell, surrounded by abundant mitochondria (white*) and dilated cisternae of smooth endoplasmic reticulum (SER) (white ◊). Notice the (F) flagellum; (¤) cortical cell nucleus; (●) *T. evansi* mithochondrion; (→) glycosomes. Bar: 1.2 µm.

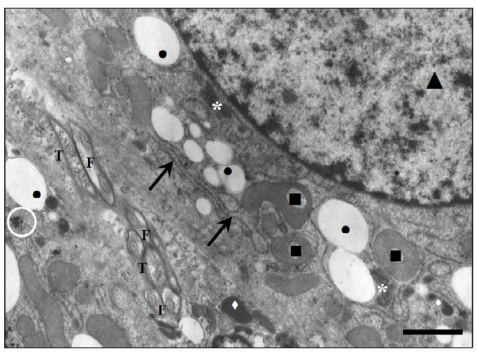

Figure 12: Oblique sections of *T. evansi* body (T) and flagella (F) inside the cytoplasm of hepatocytes (Bar: 0.8 µm). Notice the normal ultrastructure of hepatocytes characterized by nucleus (▲), lipid droplets (●), vacuolated mitochondria (■), RER (→), glycogen granules (○), lysosomes (white ♦), peroxisomes (white *).

Figure 13: Intracellular trypomastigotes of *T. evansi* (T) inside the cytoplasm of a necrotic hepatocyte (■) below the Disse's space (↔). Notice the abundance of oblique sections of *T. evansi* flagella in the hepatocyte cytoplasm, the normal ultrastructure of the trypomastigote and its proximity to lipid droplets (*), mitochondria (¤), and glycogen granules (○) from hepatocyte. (◊) sinusoid lumen; (white →) glycosomes; (●) mitochondrion; (white ▲) RER; (black ♦) acidocalcisomes; (white ♦) Golgi apparatus; (white *) nuclear envelope; (white ■) trypanosome nucleus.

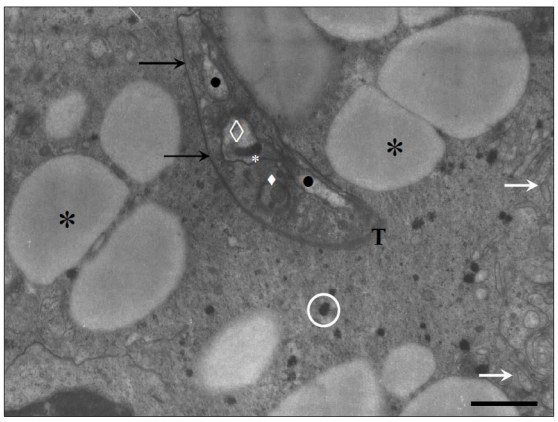

Figure 14: Intracellular form of *T. evansi* (T) inside the cytoplasm of a necrotic hepatocyte surrounded by lipid droplets (black *) and glycogen granules (○) near the Disse's space where microvilli of hepatocytes (white →) can be observed. Notice that ultrastructure of the intracellular form of *T. evansi* resembles an epimastigote stage. (◊) Kinetoplast; (white*) compacted kDNA microfibrils; (●) mitochondrion; (white ♦) Golgi complex and vesicles; (black →) trypanosome surface coat. Bar: 1.0 µm.

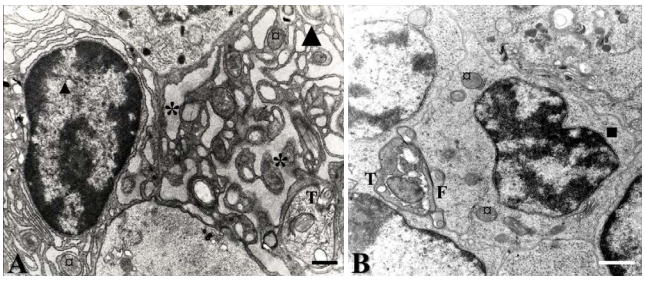

Figure 15: Intracellular trypomastigotes of *T. evansi* (T) inside the cytoplasm of **(A)** a plasma cell (▲) (Bar: 0.5 µm) and **(B)** interacting with a large activated lymphocyte (■) (Bar: 0.7 µm) of spleen white pulp from experimentally infected mice. Notice the ultrastructural feature of the plasma cell showing the nucleus (white ▲) with the typical cartwheel configuration as well as the cytoplasm with abundant dilated cisternae of RER (*) surrounding trypanosome body and flagellum (white F). (F) trypanosome flagellum; (→) trypanosome mitochondrion; (♦) trypanosome nucleus; (¤) plasma cell mitochondria.

about a feasible mechanism for the internalization of *T. evansi* in these tissues is proposed based on the results herein presented, as well as results previously published by our group [25-27,29,30] and from other authors working with *T. evansi* and other trypanosome species (Figure 16).

Discussion

The occurrence of intracellular stages of *T. evansi* is something relatively new. Only a letter to the editor, previous to our works describes the presence of amastigote and spheromastigote stages in the brain of a cat infected with *T. evansi* [36]. This communication contrasts with findings reported to the date about morphology of trypanosomes of subgenus *Trypanozoon* (Salivary Section). It is important to highlight that with the exception of the epimastigote-like stage that was herein presented; all of the intracellular trypanosomes detected in our work were trypomastigotes. Moreover, in all of studied samples we have not observed the presence of trypomastigotes in different stages of rolling as it has been described by Ormerod and Venkatesan [37] for *T. brucei*. In addition trypomastigotes were observed freely in the cytoplasm and not enclosed in a parasitophorus vacuole, as it has been described for *Leishmania* spp and the initial stages of infection of cardiomyocytes with *T. cruzi* [38].

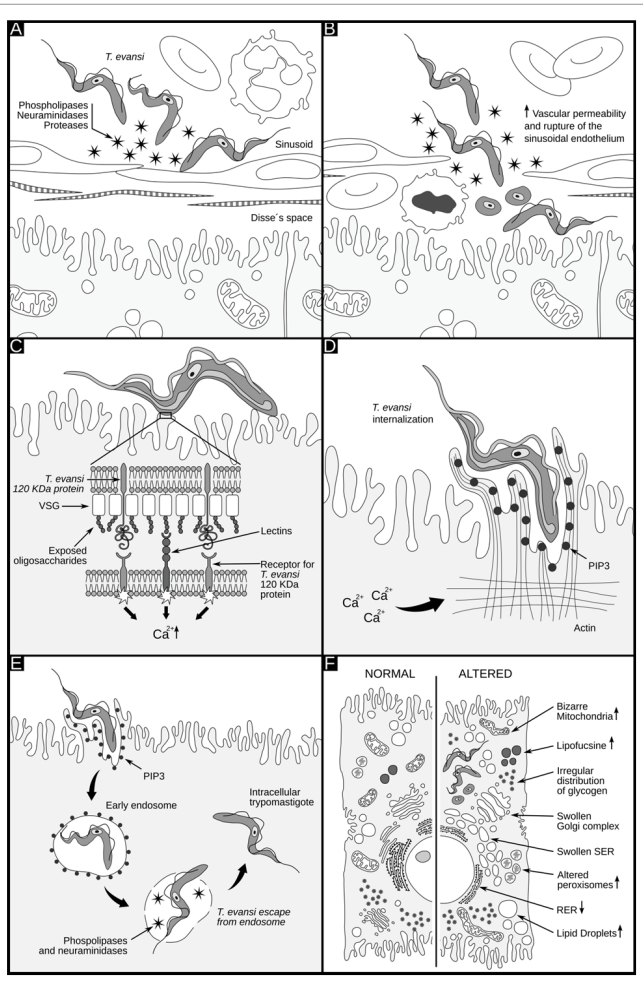

Figure 16: Working hypothesis about a feasible mechanism for the invasion of host cells in the experimental infections of mice *T. evansi* EcHF91, upon the basis of results herein presented as well as other findings of our group and researchers working with *T. evansi* and other trypanosome species Rossi et al. [25]; Finol et al. [26]; Rossi et al. [27]; Finol and Roschman [29]. de Souza et al. [38]; Anosa and Kaneko [47]; Esievo and Saror [48]; Giardina et al. [49]; Knowles et al. [50]; Tizard et al. [51]; Poltera [52]; Igbokwe [53]; Banks [55]; Jenkins [56]; Ming et al. [57]; Moody et al. [58]; Vray et al. [59]; Kleshchenko et al. [60]; Frazier and Glaser [61]; Turner and Donelson. [62]; Shehu et al. [63]; Rossi et al. [64]; Zhao et al. [65]; Grab et al. [66]; Nikolskaia et al. [67]; Nikolskaia et al. [68]; Scharfstein et al. [69]; Samad et al. [70]; Nok et al. [71]. (↑) increase; (↓) decrease.

This observation previously reported for *T. brucei* in the CNS of infected rats and mice [39-42], was described for the very first time for *T. evansi* by our group [25] as a casual finding during studies about the ultrastructural pathology in murine infected with this trypanosome. From the year 1999 to the date, we have accumulated more substantial ultrastructural evidences about the occurrence of this phenomenon in the experimental infections of albino mice with EcHF91 isolate.

Studies performed by our group (manuscript in preparation) with other Venezuelan isolates of *T. evansi*, such as the isolated *HhHF92* from a Venezuelan capybara (*Hydrochoerus hydrochaeris*) captured in 1992 at the same locality of the EcHF91 isolated, and *EcM96* isolated from an infected horse at Mantecal (Apure state) in 1996, not only have demonstrated differences in the parasitological behavior, but also the inability to develop this intracellular stages in albino mice experimentally infected, results that were in agreement with studies performed with different isolates of *T. evansi* [43-45], in which it was impossible to detect the presence of intracellular trypanosomes.

Although we have found trypomastigotes of *T. evansi* inside necrotic spaces lacking of plasma membrane limits, we have also detected intracellular trypomastigotes inside spaces with membrane limits that show a normal looking ultrastructure in adrenal cortex cells, hepatocytes, endothelial cells and plasma cells. In these spaces trypanosomes observed, show the typical ultrastructural features of trypanosomes belonging to the subgenus *Trypanozoon* as it has been described for a Venezuelan isolate of *T. evansi* [35] and for African trypanosomes belonging to brucei-group [46]. In all of the cases trypanosomes were surrounded by mitochondria, lipid droplets, glycogen granules and RER with normal ultrastructure.

The appearance of intracellular trypomastigotes in the cytoplasm of these cells should be a consequence of mechanisms responsible for the increased vascular permeability, as well as necrotic process and large gaps seen in the endothelial walls [25,27], together with the presence of receptors to *T. evansi* surface ligands in the affected host cells. The mechanism through which *T. evansi* infects or penetrates these cells is unknown, however this event would be explainable if an active invading process mediated by parasite's biologically active molecules as well as ligands and receptors in host cells, are present.

As it can be seen in Figure 16, a working hypothesis about a feasible mechanism for the internalization of *T. evansi* in these tissues is proposed according to the results herein presented, and other published by our group [25-27,29-30], as well as from other authors working with *T. evansi* and other trypanosome species. It is important to clarify that the working hypothesis never intends to assert that intracellular forms described in this paper occur as described in the figure. This hypothesis should be tested through experimentation.

According to Figure 16A, in the first step, the secretion or releasing of different trypanosome enzymes (proteases, peptidases, phospholipases, etc.) to the bloodstream during the infection, could act in a synergistic way causing damages of the sinusoid walls, vascular endothelium, blood cells and tissues as it has been described for *T. brucei* [47] and *T. vivax* [48]. In addition a 29 kDa *T. evansi* cysteine-proteinase with gelatinolytic activity, secreted extracellulary [30] and detected as a

somatic antigen in trypomastigotes of *T. evansi* and *T. equiperdum* [49], could act by removing sialic acid residues in the form of glycopeptides [50], which along with trypanosomal phospholipases can induce vasculitis and an increase of the vascular permeability [51-53].

On the other hands, the high levels reached by these antigens from trypanosomes in bloodstream and its reactions with specific antibodies and complement, could be responsible for the formation of immune complexes [54] to produce tissue damages and inflammation due the release of kallikrein that together with phospholipases, are capable to activate kininogen to produce bradykinin and kallidin, which in turn increases vascular permeability by combining with acidic groups from mucopolysaccharides and endothelial glycoproteins [53].

The interaction of *T. evansi* with the endothelial cells in addition to the necrotic process, the large gaps seen in the capillary walls [25,26] and liver sinusoids [27], and the mechanic effects associated to the motility of trypanosomes [55,56], could explain the presence of trypanosomes and blood cells in the Disse`s and sub-endothelial spaces of liver and adrenal cortex, but also the interaction of trypanosomes with the parenchymatous cells of these tissues (Figure 16B). In the hypothetic process proposed, the interaction-invasion of host cells by *T. evansi* can be divided into three stages: adhesion and recognition, signaling, and invasion. As it has been described for *T. cruzi* entry process, many molecules that are present in the membrane of the host cells such as lectins and bradykinin receptors, could be potential partners for recognition depending on the cell type involved [38].

Lectins present in mammalian cells are represented by sugar-binding proteins, which are highly specific for their sugar moieties and are involved in attachment between pathogens and host cells [57-60]. In a second step, presence of lectins on the plasma membrane of these cells, as it has been described for hepatocytes and Küpffer cells [61] could help the adhesion of *T. evansi* to endothelial cells, cells of the adrenal cortex, plasma cells and lymphocytes. These evidences are supported by findings about the binding of murine hepatocytes to acrylamide sheets containing D-galactose, one of the most abundant monosaccharides on the Variable Surface Glycoprotein of the surface coat of African trypanosomes [62]. On the other hand, secretion of sialidases whose levels are marked increased in plasma of bucks experimentally infected with African isolates of *T. evansi* [63], could produce cleavage of surface sialic acids from host cells, exposing β-galactosyl residues which in turn could be breakdown by β-galactosidase or been recognized by β- D-galactose specific lectins on the surface of adrenal cortex cells, hepatocytes, white blood cells, macrophages and Küpffer cells from hepatic sinusoids, leading to the adhesion of *T. evansi* to host cells and the abnormal extravascular erythrophagocytosis observed during experimental infections of mice [64].

This first interaction could be stabilized by the specific recognition of a 120 kDa *T. evansi* protein, through cell surface receptors as it has described for peritoneal macrophages, lymphocytes and epithelial cells from mice kidney (Zhao et al., unpublished data), and presented at the First International Seminar on Non Tsetse-Transmitted Animal Trypanosomosis in Annecy (France) in October 14-16, 1992 [65].

During adhesion-recognition process, these interactions parasite-host cells could also represent external signals which are transduced intracellularly determining a cell signaling event with the consequent increase on intracellular calcium ions level (Ca^{2+}) (Figure 16C) as it has been described for *T. cruzi*.

The intracellular calcium levels may also remain high by the effect of the 29 kDa cysteine-protease secreted by *T. evansi* [30]. This protease could stimulate an influx of Ca^{2+} that determine the invasion of the cells, in a similar way described for the brucipain, a 30 kDa cysteine-protease released during the infection of the CNS cells and endothelial cells with *T. brucei gambiense* [66-68].

The bradykinin receptors are another class of receptors that *T. evansi* could use to penetrate host cells, as it has been described for the invasion of Chinese hamster ovary (CHO) cells by *T. cruzi* trypomastigotes. These receptors are coupled to the heterotrimeric protein G and are formed by two subtypes: the bradykinin-2 receptor, which is constitutively, expressed by cardiovascular cells and the bradykinin-1 receptor whose expression is up-regulated in injured tissues [69].

The invasion of host cells by *T. evansi* could be achieved by the actin dependent pathway (Figure 16D). According to this pathway, trypomastigotes penetrate into a host cell through plasma membrane expansions and invaginations that accumulates phosphoinositol triphosphate (PIP3), a phosphoinositide which is produced by class I PI3 Kinase, as a consequence of the increase in the intracellular levels of Ca^{2+} [38]. This event culminates with the assembly of a parasitophorous vacuole formed from the plasma membrane containing internalized *T. evansi* trypomastigotes (Figure 16E). Subsequently, trypomastigotes could produce the lysis of the parasitophorous vacuole membrane (Figure 16E) through the releasing of phospholipases [70], and/or the action of a membrane-bound neuraminidase that was isolated from bloodstream trypomastigotes of *T. evansi* [71].

The enzymatic breakdown of the parasitophorus vacuole, could lead to the presence of free *T. evansi* trypomastigotes in the cytoplasm of cells exhibiting different degrees of ultrastructural alterations, as it has been described in previous works (Figure 16F) [25-27,29].

The intracellular stages of *T. evansi* could be one of the many biological characters shared by particular genotypes of trypanosomes belonging brucei-group [31,72] and capable to develop cryptic stages [37,39,41], as it has been described for their ultrastructure, their mammalian hosts, way of transmission, pathogenicity, biochemical [49] and molecular characteristics.

From the biological and pathological point of view, these intracellular trypomastigotes could be implicated as a source of relapse after chemotherapy [40,72] and must contribute seriously to the pathogenesis of the infection by producing direct and indirect ultrastructural alterations of liver, adrenal cortex, vascular endothelium, red blood cells [25-27,64], as well as immunosuppression as a consequence of its tropism for lymphocytes and plasma cells. These are important facts to be considered by research groups that are working on the development of new drugs against *T. evansi*, especially if drugs cannot cross the plasma membrane of the infected host cells.

In addition, intracellular trypomastigotes could be responsible for the recolonization of the vascular bed once the first VAT's was destroyed by specific antibodies, as it has been proposed by Seed et al. [73] for antigenic variation during experimental infections of *Microtus montanus* with *T. brucei gambiense* (Wellcome TS strain).

As it has been described for *T. brucei*, the occurrence of intracellular stages of *T. evansi* EcHF91 in the murine models could be explained as a capability or peculiarity of this genotype of *T. evansi*, because these intracellular stages it has not been described yet in other Venezuelan isolates of *T. evansi* studied such as *EcM96*, *HhHF92* and *TEVA1*.

On the other hand, because the invasion process could be determined by the size of the developing trypanosome population and the induction of the overexpression of receptors for parasite

surface macromolecules, as it has been described for the Low Density Lipoprotein receptor (LDLr) overexpression in cardiac cells of mice experimentally infected with *T. cruzi* [74], more assays should be performed in order to determine if the invasion process constitute an parasitaemia-associated event during the experimental infection with the isolated EcHF91.

Regarding to programed cell death in pathogenic trypanosomatids, it has been described for *T. cruzi* [75], *L. amazonensis* [76] and *T. brucei* [77,78], showing ultrastructural and biochemical profiles similar to those described in apoptotic processes [79].

In the intracellular trypomastigote stages of *T. evansi* described in this work, the ultrastructural apoptotic features detected were similar to those described by Barth et al [78] in *T. brucei* staurosporine-induced cell death such as significant increase in glycosomes, acidocalcisomes and lysosomes number and electron density, increase in flagellar pocket size and volume, appearing of vesicles and constrictions inside the flagellar pocket among other.

Because pathogenic trypanosomatids are able to induce apoptotic responses in the populations of parasitized host cells, but also in their own populations during the course of infection [79,80], apoptosis must surely be playing an important role in the host-parasite relationship. In this sense, parasitic apoptosis seems to be involved in the evasion of host's inflammatory response (inhibiting or promoting their survival), as well as in the auto regulation of the uncontrolled growth of parasitic population, to avoid the early death of host and thus contribute to maximize their own dispersion and survival [79,81].

The occurrence of these intracellular stages in susceptible hosts under natural or field conditions could have important consequences at epidemiological level. In this regard, they could be responsible for cryptic parasitaemia described during infections of bovines [9], but also of the high levels of prevalence (30-50%) that could only be revealed by PCR in areas where the *T. evansi* infection is enzootic [10].

More research is needed not only to demonstrate the occurrence of these stages in horses, cattle, bubaline and capybara under field conditions, but also to know the mechanisms through which *T. evansi* invades host cells, as well as to assess the correlation of its presence with the high levels of prevalence in enzootic areas

Acknowledgements

Authors would like to thank the Histotechnologist Beatriz Bello for her invaluable technical assistance in the transmission electron microscopic studies and to the technicians of the animal facilities (Instituto de Biología Experimental, Facultad de Ciencias, Universidad Central de Venezuela; IBE-UCV) for their invaluable assistance and maintenance of experimental animals.

Conflict of Interest

"The authors (Marcello S. Rossi S.; Alpidio Alejandro Boada-Sucre; María Lorena Márquez; Pedro Rodríguez; María Gilma Hernández; Francisco García; Gilberto Payares; Héctor J. Finol) declare that there is no conflict of interest regarding the publication of this article."

References

1. Kristjanson PM, Swallow BM, Rowlands GJ, Kruska RL (1999) Measuring the costs of African animal trypanosomosis, the potential benefits of control and returns to research. Agr Syst 59: 79-98.
2. Swallow BM (2000) Impacts of trypanosomosis on African agriculture. In: Watanabe, S. (ed.) PAAT Technical and Scientific Series Rome, pp. 2.
3. Department for International Development (2001) Trypanosomosis, tsetse and Africa. The year 2001 report. Department for International Development, Aylesford, UK.
4. Rangel R (1905) Nota Preliminar sobre la Peste Boba y Derrengadera de los Equinos de los Llanos de Venezuela (Trypanosomiasis). Gac Méd Caracas 12: 105-113.
5. Reyna-Bello A, García FA, Rivera M, Sansó B, Aso PM (1998) Enzyme-linked immunosorbent assay (ELISA) for the detection of anti-*Trypanosoma evansi* equine antibodies. Vet Parasitol 80: 149-157.
6. Raymond HL (1990) *Tabanus importunus*, experimental mechanical vector of *Trypanosoma vivax* in French Guiana. Ann Parasitol Hum Comp 65: 44-46.
7. Otte MJ, Abuabuara JY (1991) Transmission of South American *Trypanosoma vivax* by the neotropical horsefly *Tabanus nebulosus*. Acta Trop 49: 73-76.
8. Coronado A, Suarez C, Román D (2006) Survival of *Trypanosoma evansi* in the intestinal tract of experimentally infected *Stomoxys calcitrans*. Gac Cienc Vet 12: 72-76.
9. Rossi S MS, Aso PM, García F (2018) Assessment of Parasitological Behaviour, Clinical Changes and Serology during Experimental Infection of a Calf with a Venezuelan Isolate of *Trypanosoma evansi*: A Preliminary Study. Diagn Pathol Open 2: 125.
10. Ramírez-Iglesias JR, Eleizalde MC, Reyna-Bello A, Mendoza M (2018) Molecular diagnosis of cattle trypanosomes in Venezuela: evidences of *Trypanosoma evansi* and *Trypanosoma vivax* infections. J Parasit Dis 41: 450-458.
11. Arias JF, García F, Rivera M, López R (1997) *Trypanosoma evansi* in capybara from Venezuela. J Wildlife Dis 33: 359-361.
12. Joshi PP, Shegokar VR, Powar RM, Herder S, Katti R, et al. (2005) Human Trypanosomiasis caused by *Trypanosoma evansi* in India: The First Case Report. Am J Trop Med Hyg 73: 491-495.
13. Powar RM, Shegokar VR, Joshi PP, Dani VS, Tankhiwale NS, et al. (2006) A rare case of human trypanosomiasis caused by *Trypanosoma evansi*. Indian J Med Microbiol 24: 72-74.
14. Infectious Disease Society of America (2016) First reported human infection with the zoonotic parasite *Trypanosoma evansi* in Southeast Asia. Outbreak News Today, For Oxford University Press.
15. Truc P, Büscher P, Cun G, Gonzatti MI, Jannin J, et al. (2013) Atypical Human Infections by Animal Trypanosomes. PLoS Negl Trop Dis 12: e2256.
16. Luckins AG (1988) *Trypanosoma evansi* in Asia. Parasitol Today 4: 137-142.
17. Hörchner F, Syakalima M, Wust B (1983) Experimental Infection of Horses with *Trypanosoma evansi*. Parasitological and Clinical Results. Ann Soc Belg Med Trop 63: 127-135.
18. Sudarto MW, Tabel H, Haines DM (1990) Immunohistochemical Demonstration of *Trypanosoma evansi* in Tissues of Experimentally Infected Rats and a Naturally Infected Water Buffalo (*Bubalus bubalis*). J Parasitol 78: 422-424.
19. Luckins AG, McIntyre N, Rae PF (1992) Multiplication of *Trypanosoma evansi* at the site of infection in skin of rabbits and cattle. Acta Trop 50: 19-27.
20. Uche UE, Jones TW (1992) Pathology of experimental *Trypanosoma evansi* infections in rabbits. J Comp Pathol 106: 299-309.
21. Quiñones-Mateu ME, Finol HJ, Sucre LE, Torres S (1994) Muscular Changes in Venezuelan Wild Horses Naturally Infected with *Trypanosoma evansi*. J Comp Pathol 110: 79-89.
22. Tuntasuvan D, Mimapan S, Sarataphan N, Trongwongsa L, Itraraska R, et al. (2000) Detection of *Trypanosoma evansi* in brains of the naturally infected hog deer by streptavidine-biotin immunohistochemistry. Vet Parasitol 87: 223-230.
23. Biswas D, Choudhury A, Misra KK (2001) Histopathology of *Trypanosoma (Trypanozoon) evansi* Infection in Bandicoot Rat. I. Visceral Organs. Exper Parasitol 99: 148-159.
24. Losos GJ, Ikede BO (1972) Review of Pathology of the Diseases in Domestic and Laboratory Animals caused by *Trypanosoma congolense*, *T. vivax*, *T. brucei*, *T. rhodesiense* and *T. gambiense*. Vet Pathol 9: 16-19.
25. Rossi M, Boada-Sucre AA, Finol HJ, Tejero F, Bello B, et al. (1999) Ultrastructural alterations in the adrenal gland cortex of mice experimentally infected with a Venezuelan isolate of *Trypanosoma evansi*. J Submicrosc Cytol Pathol 3: 509-513.
26. Finol HJ, Boada-Sucre AA, Rossi M, Tejero F (2001) Skeletal muscle ultrastructural pathology in mice infected with *Trypanosoma evansi*. J Submicrosc Cytol Pathol 33: 65-71.

27. Rossi S MS, Boada-Sucre AA, Hernández G, Bello B, Finol HJ, et al. (2008) Ultra-structural Analysis of Liver in Mice Experimentally Infected with a Venezuelan Isolate of *Trypanosoma evansi* (Kinetoplastida:Trypanosomatid ae). Acta Micros 17: 5-12.

28. Goodwin LG (1970) The Pathology of African Trypanosomiasis. Trans R Soc Trop Med Hyg 64: 797-812.

29. Finol HJ, Roschman-González A (2014) Ultrastructural Study on Tissue Alterations Caused by Trypanosomatids in Experimental Murine Infection. Front Public Health 2: 75.

30. Rossi M, Bremo A, Gonzatti MI, Giardina S (1995) *Trypanosoma evansi*: secretes proteins into extracellularly. Acta Cien Venez 46: 88.

31. Brun R, Hecker H, Lun Z-R (1998) *Trypanosoma evansi* and *Trypanosoma equiperdum*: distribution, biology, treatment and phylogenetic relationship. Vet Parasitol 79: 95-107.

32. Brener Z (1962) Therapeutic activity and criterion of cure on mice experimentally infected with *Trypanosoma cruzi*. Rev Inst Med Trop Sao Paulo 4: 389-396.

33. Finol HJ, Ogura M (1977) Observaciones sobre dos tipos de fibras “twitch” en el reptil *Cnemidophorus lemniscatus*. Acta Cient Venez 28: 213-219.

34. Boada-Sucre AA, De Stefano H, González B, Soto H, Godoy S, et al. (1999) Microscopía electrónica de barrido de las alteraciones presentes en los espermatozoides de toros mestizos Siboney. Rev Cien 9: 235-242.

35. Hernández-Páez R (1980) Consideraciones Ultraestructurales sobre el *Trypanosoma venezuelense*, Mesnil 1910: Aspecto Morfológico Normal del *Trypanosoma venezuelense*. Rev Fac Ciens Vet UCV 28 83-106.

36. Choudhury AY, Misra KK (1973) Occurrence of amastigote and sphaeromastigote stages of *Trypanosoma evansi* in the brain tissue of the cat. Trans R Soc Trop Med Hyg 67: 609.

37. Ormerod WE, Venkatesan S (1971) An amastigote Phase of the Sleeping Sickness. Trans R Soc Trop Med Hyg 65: 736-741.

38. W de Souza, TMU de Carvalho, ES Barrias (2010) Review on *Trypanosoma cruzi*: Host Cell Interaction. Int J Cell Biol 29: 5394

39. Ormerod WE, Venkatesan S (1971) The Occult Visceral Phase of Mammalian Trypanosomes with Special Reference to the Life Cycle of *Trypanosoma Trypanozoon brucei*. Trans R Soc Trop Med Hyg 65: 722-735.

40. Jennings FW, Whitelaw DD, Holmes PA, Chizyuka HGB, Urquhart HGM (1984) The brain as a source of relapsing *Trypanosoma brucei* infection in mice after chemotherapy. Int J Parasitol 9: 381-384.

41. Ormerod WE (1984) Regeneration of ependymal cells of the choroid plexus with *Trypanosoma brucei*. Trans R Soc Trop Med Hyg 78: 275.

42. Ormerod WE, Hussein MS (1986) The ventricular ependyma of mice infected with *Trypanosoma brucei*. Trans R Soc Trop Med Hyg 80: 626-633.

43. Tejero F, Brun S, Roschman-Gonzalez A, Velasco E, Aso PM, et al. (2009) Ultraestructura renal en infecciones murinas experimentales con un aislado venezolano de *Trypanosoma evansi*. INHRR 40: 44-49.

44. Tejero F, Arias-Mota LL, Roschman-González A, Aso PM, Finol HJ (2010) *Trypanosoma evansi*: ultrastructural cardiac muscle and cardiac microvasculature changes in experimental murine infections. Acta Sci Vet 38: 279-285.

45. Tejero F, Brun S, Roschman-Gonzalez A, Perrone-Carmona TM, Aso PM, et al. (2009) *Trypanosoma evansi*: Analysis of the ultrastructural changes in hepatic cells during murine experimental infections. Acta Micro 18: 28-32.

46. Vickerman K, Preston TM (1976) Comparative Cell Biology of the Kinetoplastida Flagellates. In: W.H.R. Lumsden and D.A. Evans, (eds) Biology of the Kinetoplastida. Academic Press, London, pp: 35-130.

47. Anosa VO, Kaneko JJ (1983) Pathogenesis of *Trypanosoma brucei* infection in deer mice (*Peromyscus maniculatus)*: Light and electron microscopic studies on erythrocyte pathologic changes and phagocytosis. Am J Vet Res 44: 645-651.

48. Esievo KAN, Saror DI (1991) Immunochemistry and immunopathology of animal trypanosomiasis. Vet Bull 61: 213-219.

49. Giardina S, Paganico G, Urbani G, Rossi M (2003) A Biochemical and Immunological Comparative Study on *Trypanosoma equiperdum* and *Trypanosoma evansi*. Vet Res Comm 27: 289-300.

50. Knowles G, Abebe G, Black SJ (1987) Peptidase in the plasma of mice infected with *Trypanosoma brucei brucei*. Parasitology 95: 291-300.

51. Tizard IR, Imes WL, Nielsen KH (1978) Mechanism of the anemia in trypanosomiasis: studies on the role of the hemolytic fatty acids derived from *Trypanosoma congolense*. Tropenmed Parasit 29: 108-114.

52. Poltera AA (1985) Pathology of human African trypanosomiasis with reference to experimental African trypanosomiasis and infections of the central nervous system. British Med Bull 41: 169-174.

53. Igbokwe IO (1994) Mechanism of cellular injury in african trypanosomiasis. Vet Bull 64: 611-620.

54. Losos GJ (1986) Infectious Tropical Diseases of Domesticated Animal Infectious tropical diseases of domestic animals. Biochem 48: 318.

55. Banks KL (1978) Binding of *Trypanosoma congolense* to the Walls of Small Blood Vessels. J Protozool 25: 241-245.

56. Jenkins GC (1980) Effects of trypanosomes on the haemopoietic system. Trans R Soc Trop Med Hyg 74: 268-270.

57. Ming M, Ewen ME, Pereira EA (1995) Trypanosome invasion of mammalian cells requires activation of the TGF-β signaling pathway. Cell 82: 287–296.

58. Moody TN, Ochieng J, Villalta F (2000) Novel mechanism that *Trypanosoma cruzi* uses to adhere to the extracellular matrix mediated by human galectin-3. FEBS Letters 470: 305-308.

59. Vray B, Camby I, Camby I (2004) Up-regulation of galectin-3 and its ligands by *Trypanosoma cruzi* infection with modulation of adhesion and migration of murine dendritic cells. Glycobiology 14: 647–657.

60. Kleshchenko YY, Moody TN, Furtak VA, Ochieng J, Lima MF, et al. (2004) Human galectin-3 promotes *Trypanosoma cruzi* adhesion to human coronary artery smooth muscle cells. Infect Immun 72: 6717–6721.

61. Frazier W, Glaser L (1979) Surface components and cell recognition. Ann Rev Biochem 48: 491-523.

62. Turner MJ, Donelson JE (1990) Cell Biology of African Trypanosomes. In: D.J Wyler (ed), Modern Parasite Biology. Cellular, Immunological and Molecular Aspects, W.H. Freeman and Company, New York, pp: 51-63.

63. Shehu SA, Ibrahim NDG, Esievo KAN, Mohammed G (2006) Neuraminidase (Sialidase) Activity and its Role in Development of Anemia In *Trypanosoma evansi* Infections. J Appl Sci 6: 2779-2783.

64. Rossi S MS, Boada-Sucre AA, Simoes MT, Boher Y, Rodríguez P, et al. (2018) Adhesion of *Trypanosoma evansi* to Red Blood Cells (RBCs): Implications in the Pathogenesis of Anemia and Evasion of Immune System. Diagn Pathol Open Open 2: 122.

65. Zhao JZ, Xu JX, Liu Z (1992) Attachment of *Trypanosoma evansi* to mouse cells. In: Proceedings of the First International Seminar on Non-TseTse Transmitte Animal Trypanosomoses. Biomed Res Int 6: 2779-2783.

66. Grab DJ, Nikolskaia O, Kim YV, Lonsdale-Eccles JD, Ito S, et al. (2004) African trypanosome interactions with an *in vitro* model of the human blood-brain barrier. J Parasitol 90: 970-979.

67. Nikolskaia OV, de A Lima AP, Kim YV, Lonsdale-Eccles JD, Fukuma T, et al. (2006) Blood-brain barrier traversal by African trypanosomes requires calcium signaling induced by parasite cysteine protease. J Clin Invest 116: 2739-2747.

68. Nikolskaia OV, Kim YV, Kovbasnjuk O, Kim KJ, Grab DJ (2006) Entry of *Trypanosoma brucei gambiense* into microvascular endothelial cells of the human blood-brain barrier. Int J Parasitol 36: 513-519.

69. Scharfstein J, Schmitz V, Schmitz V (2000) Host cell invasion by *Trypanosoma cruzi* is potentiated by activation of bradykinin B2 receptors. J Exper Med 192: 1289-1299.

70. Samad A, Licht B, Stalmach ME, Mellors A (1988) Metabolism of phospholipids and lysophospholipids by *Trypanosoma brucei*. Mol Biochem Parasitol 29: 159-169.

71. Nok AJ, Nzelibe HC, Yako SK (2003) *Trypanosoma evansi* sialidase: surface localization, properties and hydrolysis of ghost red blood cells and brain cells implications in trypanosomiasis. Z Naturforsch 58: 594-601.

72. Vickerman K (1985) Developmental Cycles and Biology of Pathogenic Trypanosomes. Brit Med Bull 41: 105:114.

73. Seed JR, Edwards R, Sechelsky J (1984) The Ecology of the Antigenic

Variation. J Protozool 31: 48-53.

74. Nagajyothi F, Weiss LM, Silver DL, Desruisseaux MS, Scherer PE, et al. (2011) *Trypanosoma cruzi* utilizes the host low density lipoprotein receptor in invasion. PLoS Negl Trop Dis 5: e953.

75. Ameisen JC, Idziorek T, Billaut-Mulot O, Loyens M, Tissier JP, et al. (1995) Apoptosis in a unicellular eukaryote (*Trypanosoma cruzi*). Implication for the evolutionary origin and role of programmed cell death in the control of cell proliferation, differentiation and survival. Cell Death Differ 2: 35-53.

76. Moreira ME, Del Portillo HA, Milder RV, Balanco JM, Barcinski MA (1995) Heat stock induction of apoptosis in promastigotes of the unicellular organism *Leishmania amazonensis*. J Cell Phy 167: 305-313.

77. Welburn SC, Dale C, Ellis D, Beecroft R, Paerson TW (1996) Apoptosis in procyclic *Trypanosoma brucei rhodesiense in vitro*. Cell Death Diff 3: 229-236.

78. Barth T, Bruges G, Meiwes A, Mogk S, Mudogo CN, et al. (2014) Staurosporine-Induced Cell Death in *Trypanosoma brucei* and the Role of Endonuclease G during Apoptosis. Open J Apoptosis 3: 16-31.

79. De Souza EM, Menna-Barreto R, Araújo-Jorge T, Kumar A, Hu Q, et al. (2006) Antiparasitic activity of aromatic diamidines is related to apoptosis-like death in *Trypanosoma cruzi*. Parasitology 133: 75-79.

80. de Souza EM, Araujo-Jorge TC, Baili C, Lansiaux A, Batista MM, et al. (2003) Host and parasite apoptosis following *Trypanosoma cruzi* infection *in vitro* and *in vivo* models. Cell Tiss Res 314: 223-235.

81. Welburn SC, Macleod E, Figuerella K, Duzensko M (2006) Programmed cell death in African trypanosomes. Parasitology Cambridge University Press 132: 7-18.